

Ab initio potential curves, dipole moments, and transition probabilities for the lowlying states of arsenic oxide

Aleksey B. Alekseyev, Abani B. Sannigrahi, HeinzPeter Liebermann, Robert J. Buenker, and Gerhard Hirsch

Citation: *The Journal of Chemical Physics* **103**, 234 (1995); doi: 10.1063/1.470694

View online: <http://dx.doi.org/10.1063/1.470694>

View Table of Contents: <http://scitation.aip.org/content/aip/journal/jcp/103/1?ver=pdfcov>

Published by the [AIP Publishing](#)

Articles you may be interested in

Lifetimes and transition dipole moment functions of NaK low lying singlet states: Empirical and ab initio approach
J. Chem. Phys. **109**, 6725 (1998); 10.1063/1.477350

Ab initio configuration interaction calculations of the potential curves and lifetimes of the lowlying electronic states of the lead dimer
J. Chem. Phys. **104**, 6631 (1996); 10.1063/1.471357

Ab initio potential energy curves for lowlying states of carbon disulfide
J. Chem. Phys. **100**, 7481 (1994); 10.1063/1.466892

Determination of electric dipole moments and transition probabilities of lowlying singlet states of CO
J. Chem. Phys. **99**, 2352 (1993); 10.1063/1.465250

Theoretical study of lowlying $1\Sigma^+$ and 1Π states of CO. I. Potential energy curves and dipole moments
J. Chem. Phys. **87**, 424 (1987); 10.1063/1.453587



Ab initio potential curves, dipole moments, and transition probabilities for the low-lying states of arsenic oxide

Aleksey B. Alekseyev,^{a)} Abani B. Sannigrahi,^{b)} Heinz-Peter Liebermann,
Robert J. Buenker, and Gerhard Hirsch

Bergische Universität—Gesamthochschule Wuppertal, Fachbereich 9—Theoretische Chemie, Gaussstr. 20,
D-42097 Wuppertal, Germany

(Received 20 December 1994; accepted 28 March 1995)

Relativistic effective core potentials (RECPs) are employed in the framework of spin-orbit configuration interaction method to compute potentials curves and one-electron properties for a large number of electronic states of the arsenic oxide molecule. Good agreement is noted between calculated and experimental data for the spectroscopic constants of states with T_e values at or below $40\,000\text{ cm}^{-1}$. The calculations predict that the lowest excited Λ -S state is the $\pi \rightarrow \pi^* a^4\Pi$ and it is argued that some experimental results of Kushawaha *et al.* originally thought to correspond to the $A''^2\Sigma^+ - X^2\Pi$ transition should be reassigned as $a^4\Pi - X^2\Pi$. There is general agreement that the corresponding $\pi \rightarrow \pi^* {}^2\Pi$ is the upper state in the $G_1, G_2 \rightarrow X^2\Pi$ band systems, with computed T_e values only 600 cm^{-1} smaller than observed, and discrepancies in r_e and ω_e values of 0.01 \AA and $16\text{--}20\text{ cm}^{-1}$, respectively. The $b^4\Sigma^-$ and $I^2\Phi$ Ω components are found to be the next lowest-energy states, but it is pointed out that the experimental L - F splitting is too large to be attributed to the $b_1^4\Sigma_{1/2}^- - b_2^4\Sigma_{3/2}^-$ energy difference. Strong perpendicular transitions are computed for the $A^2\Sigma^+ - X^2\Pi$ band system, and the upper state is found to undergo homogeneous perturbations by a number of neighboring states which should have important effects on the A - X vibrational intensity distribution. The $B^2\Sigma^+$ state has a large amount of Rydberg character and is the only low-lying AsO state with As^-O^+ polarity. The minimum in its potential curve appears to be almost coincident with a maximum in the $A^2\Sigma^+$ potential, leading to an onset of a break-up in the otherwise strong B - X emission intensity pattern at $v'=0$ and $N'=21$. On the basis of the present calculations an estimate for the D_0^0 value of the AsO ground state of 4.22 eV can be made, which is $\sim 0.7\text{ eV}$ smaller than the upper limit for this value given in the literature. Numerous comparisons with analogous calculated results for the heavier Group V oxides, SbO and BiO are made, allowing for a systematic evaluation of the changing role of relativistic effects with increasing atomic number of the heavy atom in this class of molecules. © 1995 American Institute of Physics.

I. INTRODUCTION

In recent work *ab initio* calculations employing a spin-orbit configuration interaction method in conjunction with relativistic effective core potentials (RECP's) have been carried out to investigate the electronic spectra of the Group V oxides SbO¹ and BiO.² The next heaviest member of this molecular series is arsenic oxide AsO, for which a relatively large amount of experimental data is known, as recently reviewed by Rai and Rai.³ One expects spin-orbit and other relativistic effects to be smaller for AsO than either of its heavier counterparts but still be quite significant, as witnessed by the 1026 cm^{-1} energy splitting of its $X^2\Pi$ ground state.^{3,4} In the two heavier oxides it is now established that the first excited Λ -S state is the $\pi \rightarrow \pi^* a^4\Pi$, with its $\Omega=5/2, 3/2$ and two $1/2$ components. As the importance of spin-orbit coupling declines through this series, it can be expected that it becomes progressively more difficult to observe emissions from this group of states, and so the fact that no definite assignment for them has been forthcoming on the

basis of experimental evidence is neither contradictory of this trend nor very surprising. Thus one of the goals of theoretical calculations for the AsO molecule should be to localize the energetic position of the $a^4\Pi$ states in order to aid in their ultimate detection by experimentalists.

The lowest-lying Λ -S state which has been observed in the AsO spectrum is the inverted $G^2\Pi$, which results from the same $\pi \rightarrow \pi^*$ excitation as $a^4\Pi$. The first evidence was provided by Callomon and Morgan,⁵ who concluded that it was responsible for perturbations in the $A^2\Sigma^+ - X^2\Pi$ band system they were studying. The first comprehensive spectroscopic observation was reported by Mrozowski and Santaram,⁶ who were able to characterize transitions from both the $\Omega=3/2$ and $1/2$ components down to $X^2\Pi$. They referred to the upper state as A' , and both designations, A' and G , are currently in use. The respective T_e values fall in the $25\,000\text{--}26\,000\text{ cm}^{-1}$ region of the spectrum, as compared to $21\,000\text{ cm}^{-1}$ in SbO and only $14\,000\text{ cm}^{-1}$ in BiO^{3,4} for the analogous transitions for these systems, from which one obtains a general impression of the gradual variation of the density of electronic states in this series, not only for the corresponding vibrational species. Otherwise a number of excited states, up to ten of them, have been found in the $30\,000\text{--}40\,000\text{ cm}^{-1}$ range of the AsO spectrum.^{3,4} Based on previous work for SbO¹ and BiO² it can be anti-

^{a)}Fellow of the Alexander von Humboldt Foundation; on leave from the Institute of Physics, St. Petersburg State University, 198904 St. Petersburg, Russia.

^{b)}Permanent address: Department of Chemistry, Indian Institute of Technology, Kharagpur—721 302, India.

pated that mostly $\pi \rightarrow \pi^*$ and $\sigma \rightarrow \pi^*$ transition are responsible. Although there is an abundance of experimental information about the corresponding band systems, a number of unanswered questions has arisen about certain aspects of the observed results, often tied up with the specific interpretation of various predissociation effects or otherwise nonradiative processes believed to be involved.

In the present study we will consider a similar set of *ab initio* CI calculations for the AsO molecule as those reported for the heavier oxides.^{1,2} The results include potential energy curves for states in the observed spectroscopic region up to their respective dissociation limits, along with the corresponding spectroscopic constants such as equilibrium bond lengths and vibrational frequencies. In addition electric dipole moments have been computed as well as the corresponding transition moments, which allow for hopefully reliable estimates of transition probabilities between such pairs of states and the radiative lifetimes of the corresponding upper states. These results should provide additional guidance for the eventual clarification of observed spectral data for this molecule.

II. DETAILS OF THE THEORETICAL TREATMENT

The basic approach employed in the present calculations is an *ab initio* spin-orbit CI with RECP's. In the present case the arsenic atom full-core RECP of Hurley *et al.*⁷ is taken, with only the 4s and 4p electrons not included in the atomic core. The oxygen potential for the 1s core electrons given by Pacios *et al.*⁸ is also employed, so that only 11 active electrons remain to be treated in the ensuing SCF and CI calculations. The (3s3p) AO Cartesian Gaussian basis recommended for use with the As RECP⁷ has been augmented with a six-component *d* function with optimized exponent of 0.40 a_0^{-2} . It was also necessary to add diffuse *s* (0.012 a_0^{-2}) and *p* (0.010 a_0^{-2}) functions to describe low-lying Rydberg states in the AsO spectrum. The oxygen portion of the AO basis is the same (4s4p1d) as employed in the earlier calculations of SbO¹ and BiO.² Considering the fact that only the valence shells of both atoms need to be treated explicitly in the present approach, the above basis set can be described as at least triple-zeta-plus polarization (TZP). All functions are primitive Gaussians, allowing for the maximum flexibility in representing the AsO charge distribution in a variety of electronic states.

An SCF calculation has been carried out at each internuclear distance considered for the $\cdots\sigma^2\pi^4$ AsO⁺ ground state. The analogous procedure has been employed for the two heavier oxides^{1,2} to take advantage of the favorable characteristics of ionic virtual orbitals in describing excited electronic states.⁹ Since transition moments need to be calculated between pairs of electronic states, it is especially convenient to employ the same orthonormal set of orbitals for expanding all such wave functions. Only the spin-independent portions of the As and O RECP's are employed in the SCF calculations. The treatment is carried out formally in the C_{2v} subgroup of $C_{\infty v}$ because of restrictions in the CI method employed. Nevertheless, the SCF orbitals themselves are found to transform to a high degree of accuracy according to the σ , π , \cdots irreducible representations of the linear point group,

TABLE I. Technical details of the MRD-CI calculations of AsO.^a

C_{2v} symm.	$N_{\text{ref}}/N_{\text{root}}$	SAFTOT/SAFSEL	$C_{\infty v}$ notation	Σc_p^2
${}^2B_{1,2}$	143/6	2 452 937/20 980	1 ${}^2\Pi$	0.9314
			2 ${}^2\Pi$	0.9370
			1 ${}^2\Phi$	0.9387
2A_1	136/7	2 430 150/27 002	1 ${}^2\Sigma^+$	0.9239
			1 ${}^2\Delta$	0.9217
			1 ${}^2\Sigma^-$	0.9316
2A_2	126/7	2 725 620/25 655	1 ${}^2\Delta$	0.9398
			1 ${}^4\Pi$	0.9384
			2 ${}^4\Pi$	0.9253
${}^4B_{1,2}$	161/6	3 292 728/31 387	1 ${}^4\Sigma^+$	0.9275
			1 ${}^4\Delta$	0.9297
			1 ${}^4\Sigma^-$	0.9300
4A_1	136/7	3 166 493/31 973	1 ${}^4\Delta$	0.9290
			1 ${}^6\Sigma^+$	0.9274
			1 ${}^6\Pi$	0.9349
4A_2	143/7	3 104 749/30 610	1 ${}^6\Sigma^-$	0.9369
6A_1	42/1	1 120 856/5 599		
${}^6B_{1,2}$	23/1	603 258/6 577		
6A_2	57/1	1 333 659/6 042		

^aThe number of selected SAFs and the Σc_p^2 values over reference configurations (for the lowest roots of each symmetry) are given for $r=3.1 a_0$. SAFTOT designates the total number of generated, SAFSEL the number of selected SAFs, N_{ref} and N_{root} refer to the number of reference configurations and roots treated, respectively.

making identification of the symmetry characteristics of the final CI many-electron wave functions relatively straightforward.

In the second stage of the calculations electronic states are generated in the $\Lambda-S$ coupling scheme, i.e., only uncoupled S^2 eigenfunctions. The multireference single- and double-excitation CI method (MRD-CI) is employed for this purpose.¹⁰ Energies, wave functions, and properties are computed for a series of internuclear distances between $r=2.6$ and $10.0 a_0$, in intervals of $0.1 a_0$ up to $r=5.0 a_0$ and at selected points beyond this distance. Reference configurations are chosen on the basis of the absolute magnitudes of their associated coefficients in the final CI wave functions for a series of electronic states. All singly and doubly excited configurations are generated with respect to this set, but a selection threshold of $T=5.0 \mu E_h$ is employed to divide them into two groups. The more strongly interacting configurations are included in the final secular equations to be solved explicitly, while the effect of the unselected configurations is taken into account by means of an energy extrapolation scheme based on perturbation theory.¹⁰ Details concerning the numbers of roots treated in the C_{2v} irreducible representations for doublet, quartet, and sextet symmetry, respectively, are given in Table I, along with the corresponding numbers of reference configurations and sizes of the generated and selected MRD-CI spaces. The $C_{\infty v}$ notation for some of the lowest-energy roots treated, as well as the sums of squared coefficients of the reference configurations Σc_p^2 in each case is also given. Note that it is not necessary to solve secular problems for both the B_1 and B_2 species since they always occur in degenerate pairs (Π , Φ , \cdots). The table CI algorithm¹¹ is employed in the computational scheme in order to afford efficient handling of the complex open-shell relationships which arise in the MRD-CI procedure. The $T=0$ energy results are also augmented with the generalized multireference Davidson correction^{12,13} in order to obtain an

accurate estimate of the AO basis limit for each root, whereby comparison with exact full CI benchmark results has indicated for systems of a similar number of valence electrons that such results should be reliable to within an error of 1–2 kcal/mol for all excited states independent of internuclear geometry.^{14,15} One-electron (diagonal and off-diagonal) properties are also computed, albeit on the basis of the (truncated) variational eigenfunctions only.

The Λ – S MRD-CI wave functions are then employed as a basis for a matrix representation of the relativistic spin-orbit Hamiltonian. For this purpose the spatial functions are multiplied with appropriate spin functions and the Wigner–Eckart theorem is employed to compute spin-orbit matrix elements between them based on results obtained for representative pairs of S^2 eigenfunctions. The estimated full CI energies are taken as diagonal Hamiltonian matrix elements, whereas the variational Λ – S wave functions are employed in the spin-orbit calculations. More details of the theoretical treatment may be found elsewhere.²

The Born–Oppenheimer approximation is assumed throughout and so the next step is to fit the relativistic CI potential curves obtained above to polynomials and then solve the corresponding nuclear-motion Schrödinger equations by numerical integration^{16,17} to obtain vibrational wave functions and energies. The electronic transition moments are also fit to polynomials for each component and averaged over appropriate pairs of vibrational functions. These results are combined with transition energy data to compute Einstein spontaneous emission coefficients.^{1,2} Special interest lies in the radiative lifetimes of individual upper-state vibrational levels which are obtained by summing over the transition probabilities to all lower-lying states and inverting.

III. POTENTIAL ENERGY RESULTS FOR Λ – S STATES

The potential curves obtained from the spin-independent CI calculations for the AsO molecule are given in Fig. 1. The density of states is notably smaller for this molecule than for either SbO¹ or BiO.² The $X^2\Pi$ ground state has the usual $\dots\sigma^2\pi^4\pi^*$ configuration and dissociates to $As(^4S_u) + O(^3P_g)$. The first Λ – S excited state is $a^4\Pi$, which also dissociates to the ground states of the respective atoms and arises from a $\pi \rightarrow \pi^*$ excitation. Its r_e value is shifted by 0.5 a_0 to the right in Fig. 1 relative to that of $X^2\Pi$, reflecting the large amount of antibonding character in the π^* MO. The latter effect is related to the fact that the AsO bonding is predominantly covalent, with the π orbital being somewhat more localized on oxygen, π^* on arsenic. As the electronegativity of the Group V atom decreases in this series, the amount of covalent character also lessens and the π^* is found to become more and more localized on the heavier atom,^{1,2} which has an important influence on the magnitude of the spin-orbit splittings in this class of molecules. It is important to note that the $\pi \rightarrow \pi^*$ 4Π state has been ignored in previous compilations of the AsO spectrum,^{3,4} similarly as in the original assignments of the SbO and BiO electronic spectra.^{1,2}

The next lowest-energy AsO Λ – S state is the most stable of the three $\pi \rightarrow \pi^*$ 2Π species. It is computed to have almost the same r_e value as the $a^4\Pi$, but it dissociates to

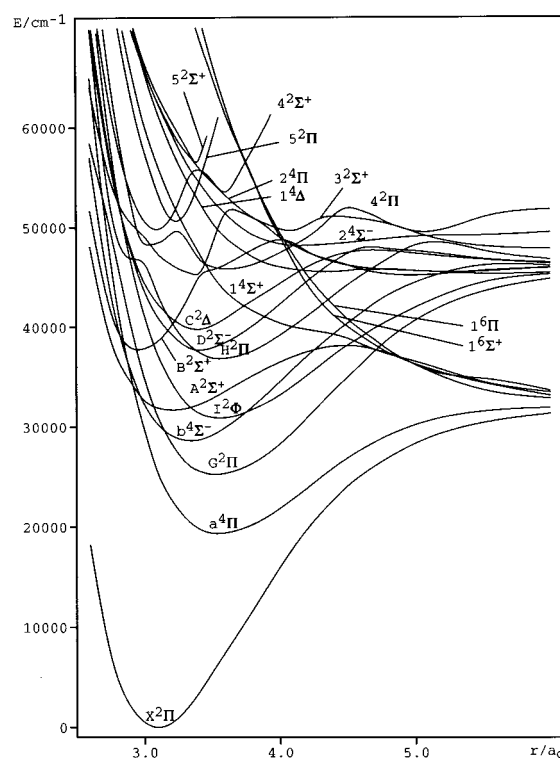


FIG. 1. Computed potential energy curves for the lowest-lying Λ – S states of the AsO molecule obtained in a theoretical treatment without the inclusion of the spin-orbit interaction.

$As(^2D_u) + O(^3P_g)$ and thus the energy splitting between them gradually increases as the bond is stretched. In the literature this 2Π state is often referred to as A' ,^{3,6} but we prefer the designation of Callomon and Morgan,⁵ namely, $G^2\Pi$. In general, it is unfortunate that the nomenclature for the Group V oxides is often inconsistent since there is usually a clear correspondence between the electronic states of AsO, SbO,¹ and BiO.² The next most stable Λ – S state according to the present calculations is the $b^4\Sigma^-$, which is the lowest state of $\sigma \rightarrow \pi^*$ type. It is easy to recognize this from Fig. 1 because of this state's relatively short r_e value, which means that the σ MO is less bonding than the π . A similar result has been found for SbO,¹ but a much smaller distinction occurs in BiO.² Shortly thereafter come the $I^2\Phi$ and $A^2\Sigma^+$ states. The former is of $\pi \rightarrow \pi^*$ type and has a very similar bond length as $a^4\Pi$ and $G^2\Pi$ (Fig. 1). It also dissociates to the second As+O limit and so the I – G energy separation gradually decreases toward large r values. A 2Φ state produces $\Omega=7/2$ and $5/2$ states, but it is somewhat difficult to observe them because of the $\Delta\Lambda$ selection rule, even though transitions to $X_2^2\Pi_{3/2}$ are dipole allowed. The $A^2\Sigma^+$ arises from a $\pi^* \rightarrow \sigma^*$ excitation and thus has only a slightly larger r_e value than the ground state. The analogous state in SbO is denoted $B^2\Sigma^+$, whereas that in BiO is called $K^2\Sigma^+$. It dissociates to the ground state atomic limits and thus possesses a definite potential energy maximum near $r=4.5 a_0$. The other such molecular states are $4,6\Sigma^+$ and 6Π , all of which have essentially repulsive potential curves

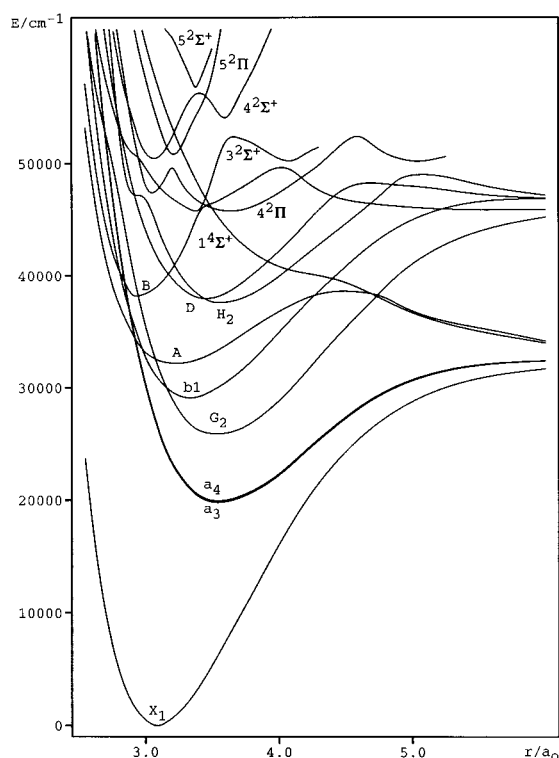


FIG. 2. Computed potential energy curves for the lowest-lying $\Omega=1/2$ states of the AsO molecule.

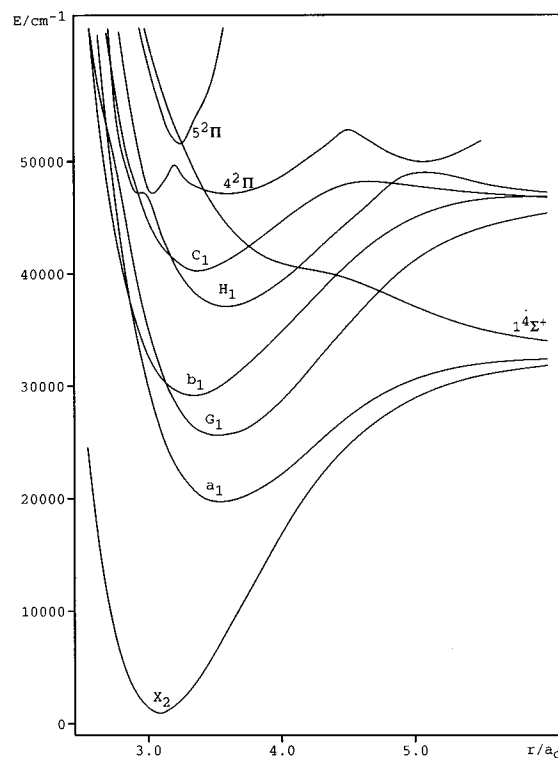


FIG. 3. Computed potential energy curves for the lowest-lying $\Omega=3/2$ states of the AsO molecule.

(Fig. 1), and therefore lie outside the Franck–Condon region of the ground state below $40\,000\text{ cm}^{-1}$.

The next group of AsO $\Lambda-S$ states are found to lie about 5000 cm^{-1} higher than $I^2\Phi$ and $A^2\Sigma^+$. The $H^2\Pi$ is the second $\pi \rightarrow \pi^*$ state of this symmetry, as can be inferred from the position of its energy minimum. Two other states in this region, $D^2\Sigma^-$ and $C^2\Delta$, arise from $\sigma \rightarrow \pi^*$ excitations, and consequently have somewhat smaller r_e values than $H^2\Pi$. The energy minimum of $B^2\Sigma^+$ lies at an even shorter bond distance than for $X^2\Pi$, since it arises from an excitation out of the antibonding π^* into a distinctly Rydberg (nonbonding) s -type orbital. The diffuse functions in the present AO basis (Sec. II) have been added with the express purpose of properly describing this state. Beyond this energy region the density of states becomes noticeably greater and several avoided crossings become apparent (Fig. 1). First, there is a third $^2\Sigma^+$ and a fourth $^2\Pi$ state, as well as $^4\Sigma^\pm$, $^4\Pi$, and $^4\Delta$ species. There are also several other low-lying $^2\Sigma^+$ states and a fifth $^2\Pi$.

IV. SPIN-ORBIT CI RESULTS AND COMPARISON WITH EXPERIMENT

Inclusion of spin-orbit coupling in the relativistic CI calculations leads to the potential energy curves which are shown in Figs. 2–6 for each of the Ω values from $1/2$ to $7/2$. Generally speaking the spin-orbit interaction does not greatly affect the shapes of the AsO potential curves, certainly much less than in SbO^1 and especially BiO^2 . Therefore, in cases where sharply avoided crossings occur between states of dif-

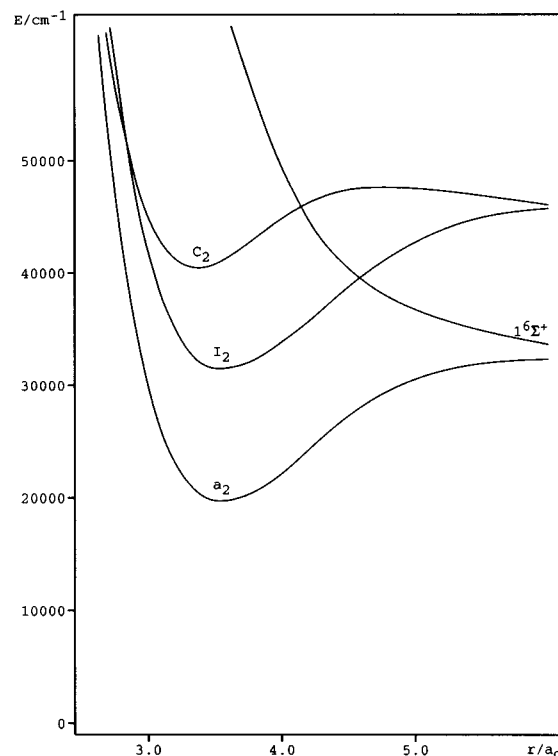


FIG. 4. Computed potential energy curves for the lowest-lying $\Omega=5/2$ states of the AsO molecule.

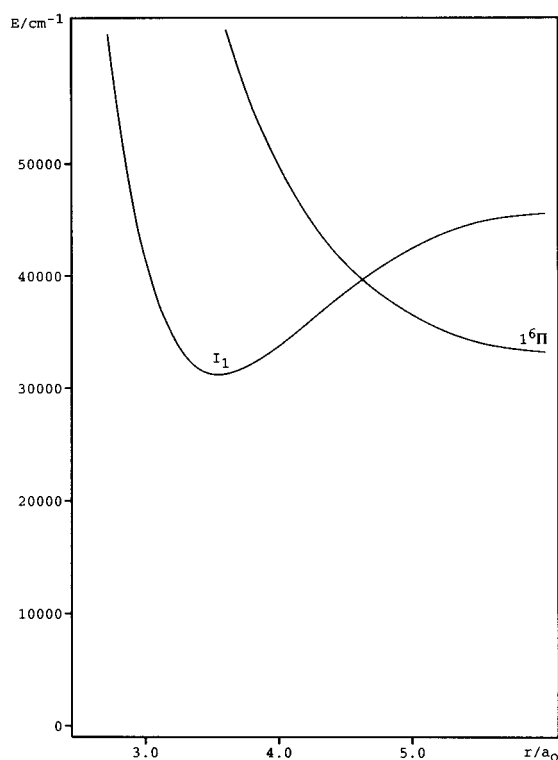


FIG. 5. Computed potential energy curves for the lowest-lying $\Omega=7/2$ states of the AsO molecule.

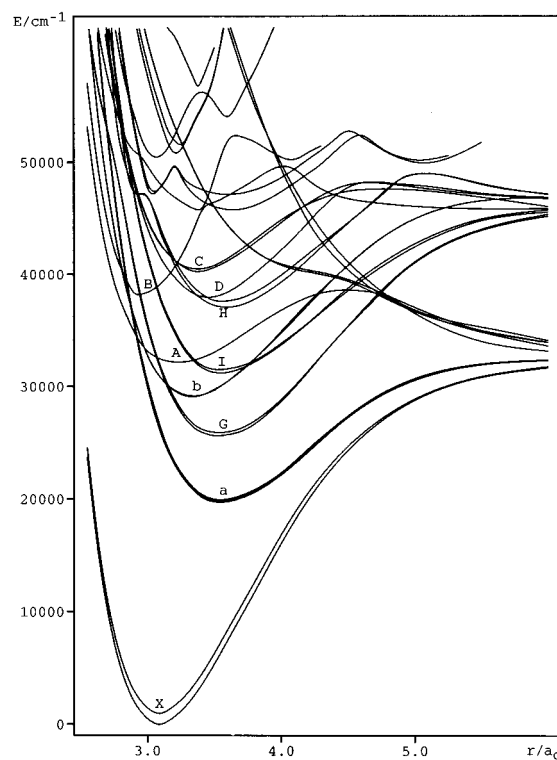


FIG. 6. Composite potential energy diagram for the low-lying Ω states of the AsO molecule.

ferent $\Lambda-S$ symmetry, the corresponding diabatic (crossing) potential curves are shown in Figs. 2–6. One should also note that the ${}^6\Sigma^+$ and ${}^6\Pi$ states have three $[1/2, 3/2, 5/2]$ and six $[1/2(2), 3/2(2), 5/2, 7/2]$ Ω components, respectively, but since all of them are repulsive and their splittings are quite small (ca. $100\text{--}300\text{ cm}^{-1}$), only components with the highest Ω value for each state are presented in Figs. 4 and 5. The computed spectroscopic constants of the lowest-lying Ω states ordered according to T_e value are given in Table II in comparison with available experimental data. The $X\ ^2\Pi$ energy splitting is underestimated by 53 cm^{-1} or about 5% in error. The r_e values of both components are found to be the same, whereby only that of the $X_1\ ^2\Pi_{1/2}$ has been determined experimentally. The computed discrepancy is 0.0064 \AA , which corresponds to an underestimation of the corresponding B_e value by 0.0036 cm^{-1} . The ω_e values computed for X_1 and X_2 are 930 and 928 cm^{-1} , which results are too low by 37 and 38 cm^{-1} , respectively. An earlier theoretical result¹⁸ overestimates the same quantity by 160 cm^{-1} and also appears to confuse the $\Delta G_{1/2}$ value with ω_e .

The four $a\ ^4\Pi$ multiplets are calculated to have T_e values just under $20\,000\text{ cm}^{-1}$ (Table II), in the order: $\Omega=3/2 < 5/2 < 1/2 < 1/2$. The analogous sequence in SbO is somewhat different, with the $5/2$ state coming in the third position.¹ The energy separation between the highest- and lowest-lying of these states is computed to be 238 cm^{-1} for AsO, as compared to 595 cm^{-1} in SbO.¹ The bond lengths are all quite similar and differ from the $X\ ^2\Pi$ values by 0.25 \AA . These states also have much smaller vibrational frequencies than those of the ground state (585 vs 930 cm^{-1} on the

average). Although no experimental assignment for the $a\ ^4\Pi$ states has yet been made, it seems likely that Kushawaha *et al.*¹⁹ have actually observed several of these multiplets in emission in what they refer to as the $A''\ ^2\Sigma^+-X\ ^2\Pi$ bands. According to the authors' evidence¹⁹ the energy available in the chemical reaction used in their study is somewhat greater than $31\,000\text{ cm}^{-1}$, which is enough to excite all low-lying states of AsO up to perhaps $A\ ^2\Sigma^+$. Thus it is necessary to consider all of these states as possible candidates for the emitting species in the observed spectrum. If the $A\ ^2\Sigma^+$ state were excited, it should have been possible to observe the strong $A-X$ emission bands, but this does not appear to have occurred. Likewise, if the upper state in question had been ${}^4\Sigma^-$, one should expect rather strong emissions to the $a\ ^4\Pi$ to be observed (see Sec. V). Still another possibility would be $I\ ^2\Phi$, but it seems quite unlikely that downward transitions to both $X\ ^2\Pi$ components could be observed in this case because of the $\Delta\Omega$ selection rule. The $G-X$ transition was also seen independently in another wavelength region. One is left with at least a reasonable alternative, namely, that the band system reported in Ref. 19 is caused by $a\ ^4\Pi-X\ ^2\Pi$ transitions. The weakness of the features observed is consistent with such spin-forbidden processes. A diffusion flame technique was applied to a mixture of AsCl_3 , O_2 , and potassium, so there is also a possibility that something entirely different is involved.

The ω_e value deduced for the upper state in the above bands is 855 cm^{-1} , which is quite high compared to the computed $a\ ^4\Pi$ values ($582\text{--}586\text{ cm}^{-1}$). There are some questions about the assignments of the various vibrational

TABLE II. Calculated and experimental spectroscopic properties of AsO (transition energies T_e , bond length r_e , and vibrational frequencies ω_e).^a

State	$T_e(\text{cm}^{-1})$		$r_e(\text{\AA})$		$\omega_e(\text{cm}^{-1})$		$B_e(\text{cm}^{-1})$	
	Calc.	Exp. ^b	Calc.	Exp. ^b	Calc.	Exp. ^b	Calc.	Exp. ^b
$X_1 \ ^2\Pi_{1/2}$	0	0	1.630	1.6236	930	967	0.4812	0.484 82
$X_2 \ ^2\Pi_{3/2}$	973	1026	1.630		928	966	0.4814	0.485 52
$a_1 \ ^4\Pi_{3/2}$	19 667		1.881		586		0.3614	
$a_2 \ ^4\Pi_{5/2}$	19 684		1.881		585		0.3616	
$a_3 \ ^4\Pi_{1/2}$	19 769		1.882		582		0.3610	
$a_4 \ ^4\Pi_{1/2}$	19 905		1.882		582		0.3610	
$G_1 \ ^2\Pi_{3/2}$	25 538	26168	1.867		617	633	0.3667	0.371 24
				1.8553				
$G_2 \ ^2\Pi_{1/2}$	25 841	26485	1.869		610	630	0.3661	0.371 83
$b_1 \ ^4\Sigma_{1/2}^-$	29 033		1.764		677		0.4110	
$b_2 \ ^4\Sigma_{3/2}^-$	29 103		1.766		686		0.4099	
$I_1 \ ^2\Phi_{7/2}$	31 230		1.878		587		0.3627	
$I_2 \ ^2\Phi_{5/2}$	31 424		1.879		585		0.3623	
$A \ ^2\Sigma_{1/2}^+$	31 985	31652	1.702	1.6631	622	687	0.4445	0.462 40
$H_1 \ ^2\Pi_{3/2}$	37 133	37054	1.886	1.8709	596	607	0.3594	
$H_2 \ ^2\Pi_{1/2}$	37 541		1.888		599		0.3589	0.365 39
$D \ ^2\Sigma_{1/2}^-$	38 236	37555	1.816	1.794	613	630	0.3879	0.397 3
$B \ ^2\Sigma_{1/2}^+$	38 308	39866	1.563	1.5764	994	1098	0.5234	0.512 84
$C_1 \ ^2\Delta_{3/2}$	40 287	38638	1.798		665		0.3955	0.402 8
$C_2 \ ^2\Delta_{5/2}$	40 322	38686	1.798	1.765	671	656	0.3954	0.416 4

^aThe most important configurations and some of the corresponding Λ -S states in the Franck-Condon region are: $\sigma^2\pi^4\pi^*$ ($1^2\Pi$), $\sigma^2\pi^3\pi^{*2}$ ($2,4,5^2\Pi$, $1^2\Phi$, $1^4\Pi$), $\pi^4\pi_R$ ($3^2\Pi$), $\sigma^2\pi^4\sigma^*$ ($1^2\Sigma^+$), $\sigma^2\pi^4\sigma_R$ ($2^2\Sigma^+$), $\sigma^2\pi^4\sigma_R^*$ ($3^2\Sigma^+$), $\sigma\pi^4\pi^{*2}$ ($4^2\Sigma^+$, $1^2\Sigma^-$, $1^2\Delta$, $1^4\Sigma^-$), $\sigma^2\pi^3\pi^*\sigma^*$ ($5^2\Sigma^+$, $2^2\Sigma^-$, $2^2\Delta$, $1^4\Sigma^+$, $1^4\Delta$, $2^4\Sigma^-$), $\sigma\pi^4\pi^*\sigma^*$ ($2^4\Pi$), $\sigma^2\pi^3\pi^*\pi_R$ ($3^4\Pi$), $\sigma^2\pi^2\pi^{*2}\sigma^*$ ($1^6\Sigma^+$), and $\sigma\pi^3\pi^{*2}\sigma^*$ ($1^6\Pi$).

^bK. P. Huber and G. Herzberg, *Molecular Spectra and Molecular Structure, Vol. 4. Constants of Diatomic Molecules* (Van Nostrand Reinhold, Princeton, 1979).

transitions, however, and thus one could explain the high ω_e value as the result of the failure to recognize that more than one (upper) electronic state is responsible for the observed findings. For example, if one adds the computed a_4 - a_1 energy splitting of 238 cm^{-1} to the presently determined ω_e value, one arrives at a sum of roughly 820 cm^{-1} , which would fit in well with the deduced ω_e value¹⁹ of 855 cm^{-1} . Examination of Table II also shows that no other ω_e result computed for any of the AsO electronic states with T_e values of $40\,000 \text{ cm}^{-1}$ or below is particularly close to the experimental values in question. If the $a^4\Pi$ - $X^2\Pi$ assignment is correct, it is necessary to change the ν'' assignments of Ref. 19 from 0-2 to 5-7 to account for the fact that the $a^4\Pi$ equilibrium distance is considerably larger than that of the $X^2\Pi$ ground state. A simple shift of five units in all the ν'' quantum numbers of Ref. 19 is not sufficient in itself to realize a satisfactory assignment for the observed bands, however, since it would mean that an energy difference (960 cm^{-1}) previously associated with the $\Delta G(1/2)$ ground state value (957 cm^{-1}) would now have to be identified with $\Delta G(11/2)$, which is 48 cm^{-1} smaller. A completely acceptable assignment of the nine bands observed does not seem possible at the present time. The situation is complicated by the fact that according to the present calculations all four different $a^4\Pi$ components lie within a 240 cm^{-1} energy interval and each of them is found to have transitions to $X^2\Pi$ of approximately equal strength (see Tables II, IV, and the discussion in Sec. V). It is also well to note that Anderson and Callomon²⁰ have questioned the vibrational assignments of Ref. 19 as well. On the basis of these considerations it

seems that the T_e value of $16\,413 \text{ cm}^{-1}$ deduced in Ref. 19 should actually correspond to a relatively high ν'' value of either five or six, which would mean that the true result is either $20\,900$ or $21\,760 \text{ cm}^{-1}$. Such a T_e value compares favorably with the present computed results for the various $a^4\Pi$ states ($19\,600$ - $19\,900 \text{ cm}^{-1}$), especially since experience indicates that the theoretical treatment employed can be expected to underestimate this quantity by 1000 - 2000 cm^{-1} in view of the greater number of open shells in the excited state wave function relative to that of $X^2\Pi$. The latter tendency has been verified in the previous study of antimony oxide,¹ for example.

The moderately strong band systems reported to have T_e values in the $26\,100$ - $26\,400 \text{ cm}^{-1}$ range (Table II) clearly arise from $G^2\Pi$ - $X^2\Pi$ transitions. First observations were made by Callomon and Morgan,⁵ while the initial quantitative spectroscopic investigation for transitions between $\nu'=0$ -3 and $\nu''=1$ -12 was reported by Mrozovski and Santaram.⁶ Additional data were obtained by Goure *et al.*²¹ and Kushawaha *et al.*¹⁹ An important point in the analysis of this band system was the recognition that no transitions from high ν' to low ν'' quantum numbers were observed, although transitions from low ν' to all ν'' species were characterized. These results implied a significant distinction in the r_e values of the participating electronic states, which is quite consistent with a $\pi \rightarrow \pi^*$ excitation process (Figs. 1-3). The present computed T_e values for G_1 and G_2 are only 600 cm^{-1} smaller than those observed (Table II). The corresponding spin-orbit splitting is 303 cm^{-1} , only 14 cm^{-1} less than the measured value, with the $\Omega=3/2$ state lying lower

($G\ ^2\Pi_i$). The analogous splittings in SbO^1 and BiO^2 are 615 and 186 cm^{-1} , respectively. The fact that the BiO value is smaller is not an exception to the general rule of rapidly increasing spin-orbit interaction with atomic number of the constituent. Quite the contrary, it comes about because the corresponding spin-orbit matrix elements are so much larger in BiO that they cause significant nonadiabatic interactions between neighboring states which move the two $^2\Pi$ components (G and H) much closer to one another than would otherwise be the case.

The bond lengths of the $\text{AsO}\ G\ ^2\Pi$ states are slightly overestimated in the present calculations (by 0.012 Å) and the corresponding ω_e values are too low by 16 and 20 cm^{-1} , respectively. The computed $a\ ^4\Pi$ values for these quantities indicate that their chemical bonds are slightly weaker than for the $G\ ^2\Pi$ states. On this basis one can predict that the experimental $a\ ^4\Pi\ \omega_e$ values should all be close to 600 cm^{-1} .

Mrozovski and Santaram⁶ were the first to notice that there are two subbands in the $G-X$ spectral region which are split by 1335 cm^{-1} , 309 cm^{-1} larger than the known X_2-X_1 splitting. On this basis they correctly concluded that only parallel transitions are involved (or at least that the corresponding perpendicular species are much weaker). We will see in the next section that this analysis conforms exactly to what is found in the present calculations. Because the X state is regular while G is inverted, this means that the corresponding 1/2–1/2 vibrational transitions occur at significantly higher energy than their 3/2–3/2 counterparts. The calculations find that $v'=0$ transitions are most probable to $v''=6-7$, whereas the experimental interpretation indicates that $v''=5-6$ are most intense. Similarly it was observed that $v'=1$ to $v''=4-5$ are strongest in this progression, as compared to $v''=5-6$ in the present calculations. Both theory and experiment agree that the maximum in the $v'=2$ series occurs for $v''=2-3$. It was also noted by Anderson and Callomon²⁰ that the $v'=9-12$ levels of the G_2 state are perturbed by high- J rovibrational states of the higher-lying $A\ ^2\Sigma^+$ state, as will be discussed subsequently.

The next higher-lying electronic states in the AsO spectrum according to the present calculations are the $b_1\ ^4\Sigma_{3/2}^-$ and $b_2\ ^4\Sigma_{3/2}^-$, but they have not yet been located experimentally. Actually three states have been reported in the corresponding energy region, namely, $E\ ^2\Pi$ at 27 461 cm^{-1} , F at 29 829 cm^{-1} , and $L\ ^2\Sigma^+$ at 31 652 cm^{-1} , with ω_e values of 705.5, 689, and 686 cm^{-1} , respectively.^{3,20,22} Based on an analogy with the PO spectrum, Rai and Rai³ concluded that the $^4\Sigma^-$ state's T_e value should fall in the 31 000 cm^{-1} range, with an ω_e value of $\sim 680\ \text{cm}^{-1}$. Comparing this prediction with the above experimental data and taking into account their relatively small energy difference and almost equal ω_e values, these authors suggested that L and F are simply the two components of the $^4\Sigma^-$ state. The present calculations find a much smaller splitting for the two $^4\Sigma^-$ states, however, only 70 cm^{-1} . Their computed ω_e values are in the 680 cm^{-1} range expected by Rai and Rai,³ but the corresponding T_e values are roughly 2000 cm^{-1} lower than their estimated value (Table II). Some underestimation is the norm for such calculations, especially for states of quartet

multiplicity, but it is probable that the true T_e values are closer to 30 000 cm^{-1} . It seems very unlikely based on the level of spin-orbit perturbations generally noted for the AsO molecule elsewhere in its spectrum, however, that the L and $F\ T_e$ values have been determined accurately if these states are actually the two $^4\Sigma^-$ components. It should be possible to detect $b\ ^4\Sigma^- - a\ ^4\Pi$ transitions once these states are populated, as will be discussed in the next section.

The $I\ ^2\Phi$ states come next in energetic order, with Ω values of 5/2 and 7/2, respectively (Figs. 4 and 5). Only perpendicular transitions to $X\ ^2\Pi$ are dipole-allowed, specifically from I_2 to X_2 . The $I_1\ ^2\Phi_{7/2}$ component is 194 cm^{-1} more stable according to the calculations, the same ordering as found for SbO .¹ To our knowledge the only spectroscopic observation of the $\pi \rightarrow \pi^*\ ^2\Phi$ state in any of the Group V oxides has been reported by Chergui *et al.*²³ for NO in a matrix environment, which is understandable on the basis of the $\Delta\Lambda=0, \pm 1$ selection rule and the fact that all lower-lying electronic states possess either Σ or Π symmetry.

The next lowest-lying state is the $A\ ^2\Sigma^+$, which does undergo strong transitions to $X\ ^2\Pi$ (see Sec. V). The present calculated T_e value is only 333 cm^{-1} higher than that observed.^{5,24} It arises from a $\pi^* \rightarrow \sigma^*$ excitation and thus has only a moderately larger r_e value than the ground state (Table II). The discrepancy for the present computed bond distance is unusually large (0.039 Å), however. The computed ω_e value is underestimated by a larger-than-average margin as well (65 cm^{-1}). A possible explanation for these errors might lie in the fact that the computed $B\ ^2\Sigma^+$ Rydberg state T_e value is $\sim 1500\ \text{cm}^{-1}$ lower than observed, which produces an overly strong interaction with the $A\ ^2\Sigma^+$ state in the calculations and, as a consequence, a lowering of the ω_e value for this state. It should also be noted that there is a more delicate perturbation of the $A\ ^2\Sigma^+$ state, namely interaction with high-lying $G\ ^2\Pi$ vibrational levels, as mentioned above. Callomon and Morgan⁵ observed 11 such perturbed levels, usually at high J , which is an indication of rotational nonadiabatic coupling as one would expect for a $^2\Sigma^+ - ^2\Pi$ interaction. The effect is not rotational predissociation of the $A\ ^2\Sigma^+$ levels, however, rather nonradiative transitions to the G_2 (bound) state (Figs. 1 and 2) which reduce the intensity of the $A-X$ emission spectrum. Since these transitions are spin-allowed (Sec. V), there must be a strong interaction to observe line broadening, which explains why only high J levels exhibit any marked effect. The same authors indicated that a $^4\Sigma$ state might also be involved in perturbations of the $v'=8$ and 10 $A\ ^2\Sigma^+$ vibrational levels, which is at least qualitatively consistent with the present calculations for $b\ ^4\Sigma^-$ (Fig. 2).

The second $\pi \rightarrow \pi^*\ ^2\Pi$ state is next in energy, with an observed T_e value of 37 054 cm^{-1} .^{3,4} Only the $H_1\ ^2\Pi_{3/2}$ value is known, but Rai and Rai³ have concluded that the $\Omega=1/2$ component lies roughly 515 cm^{-1} higher. The present calculations are in good agreement with these results (Table II). The $H_1\ T_e$ value is computed to be only 79 cm^{-1} higher than observed, and the corresponding energy splitting relative to H_2 is 408 cm^{-1} . The $H_1\ r_e$ value is found to be too large by 0.015 Å, the normal trend, and its ω_e is only underestimated by 11 cm^{-1} . At intermediate r values the

calculations find that the π^* MO takes on predominantly Rydberg character before changing back to valence type beyond $r=3.1 a_0$. It is probably difficult to observe $H_2 \ ^2\Pi_{1/2}$ because H_1-X_2 transitions are fairly strong (Sec. V) and also because the $D \ ^2\Sigma^-$ state is close by (Fig. 2). Since the initial and final states are of the same symmetry, it is to be expected that $\Delta\Omega=0$ transitions should dominate, as is found. The $D \ ^2\Sigma^-$ upper state has been characterized by several authors^{5,20,21,24} and the present calculations are again quite consistent with their findings (Table II). The T_e value is overestimated by less than 700 cm^{-1} and the r_e and ω_e values exhibit the usual trends. This state arises from a $\sigma \rightarrow \pi^*$ excitation and is closely related to the $b \ ^4\Sigma^-$ species already discussed. Nevertheless their r_e values differ by 0.05 \AA , with that of $^4\Sigma^-$ being smaller. Strong perpendicular transitions to both X_1 and X_2 have been observed. Some nonadiabatic mixing between the D and H_2 states (Fig. 2) caused by rotational coupling is undoubtedly present near the D potential minimum, which may explain part of the above distinctions between the respective Σ^- quartet and doublet spectroscopic constants.

With reference to SbO and BiO, the most unusual low-lying AsO state is $B \ ^2\Sigma^+$, with a measured T_e value of $39\,866 \text{ cm}^{-1}$.^{5,24,25} The calculations show that it is nearly a pure Rydberg state up to $r=3.4 a_0$, at which point it changes over to a $\sigma \rightarrow \pi^*$ species. Connelly²⁵ reported $B-X$ absorption bands up to $v'=5$ in 1934, and also noted some diffuseness in the intensity pattern which suggested that non-radiative transitions are also involved. Emission was later observed,⁵ but only from $v'=0$. Candidates for the perturbing state or states in this case (homogeneous mechanism) are seen from Figs. 1 and 2 to be the a_3 , a_4 , G_2 , b_1 , and A on the short-distance side of the $B \ ^2\Sigma^+$ potential curve and H_2 and D for larger bond distances. Computed spin-orbit matrix elements in the present study indicate that both the $D \ ^2\Sigma^-$ and $b_1 \ ^4\Sigma^-$ states are most likely responsible for the observed effects. The $B \ T_e$ value is underestimated by 1558 cm^{-1} (Table II), a notably greater error than for any of the lower-lying electronic states. The corresponding ω_e value is too low by 104 cm^{-1} , even though the r_e value is also underestimated, albeit by only 0.013 \AA .

The unusual character of $B \ ^2\Sigma^+$ can perhaps best be seen by analyzing its electric dipole moment. Of all the bound states considered for AsO it is the only one to possess a positive (As^-O^+) value (Table III). This is clearly because the $5s$ Rydberg orbital is strongly occupied in this state, with its dipole matrix element of $3.364 e a_0$ at the $B \ r_e$ value (meaning that its center of charge lies on the opposite side of the arsenic atom as oxygen). All other valence-orbital values are negative, with the charge center lying somewhere along the AsO bond. Some representative electric dipole moment values are shown as a function of bond distance in Fig. 7. It is seen that both the A and B dipole moments vary much more strongly than those of the other states. Both also have extrema near $r=2.9 a_0$ (1.53 \AA) and then rapidly decrease in absolute magnitude. In the case of the B state, this behavior indicates that the charge distribution of the $5s$ AO is pushed far behind the arsenic atom as the oxygen approaches relatively closely. Results are only given in Fig. 7 up to

TABLE III. Electric dipole moment values μ (in ea_0) of various states ($v=0$) of the AsO molecule calculated in the present theoretical treatment.

State	Lead.conf.	μ
$X_1 \ ^2\Pi_{1/2}$	$\sigma^2 \pi^4 \pi^*$	-1.0344
$X_2 \ ^2\Pi_{3/2}$	$\sigma^2 \pi^4 \pi^*$	-1.0242
$a_1 \ ^4\Pi_{3/2}$	$\sigma^2 \pi^3 \pi^{*2}$	-0.6772
$G_2 \ ^2\Pi_{1/2}$	$\sigma^2 \pi^3 \pi^{*2}$	-0.5680
$b_1 \ ^4\Sigma_{1/2}^-$	$\sigma \pi^4 \pi^{*2}$	-0.9803
$A \ ^2\Sigma_{1/2}^+$	$\sigma^2 \pi^4 \sigma^*$	-0.8691
$H_2 \ ^2\Pi_{1/2}$	$\sigma^2 \pi^3 \pi^{*2}$	-0.6335
$D \ ^2\Sigma_{1/2}^-$	$\sigma \pi^4 \pi^{*2}$	-1.0259
$B \ ^2\Sigma_{1/2}^+$	$\sigma^2 \pi^4 \sigma_R$	2.3302
$C_1 \ ^2\Delta_{3/2}$	$\sigma \pi^4 \pi^{*2}$	-0.8612

$r=3.4 a_0$ in this case, at which point an avoided crossing with the valence $3 \ ^2\Sigma^+$ state occurs (Figs. 1 and 2), greatly changing the character of the lower adiabatic state.

Transitions from $B \ ^2\Sigma_{1/2}^+$ to both $X \ ^2\Pi$ components are dipole allowed and the strongest in the low-energy AsO spectrum. The fact that relatively high rotational levels ($N' \geq 21$) are missing in the $B-X$ emission spectrum has led to the assertion⁵ that the D_0^0 value for AsO lies at or below 4.980 eV . Callomon and Morgan came to this conclusion in part because they assumed that a state of quartet or higher multiplicity must be responsible for such a perturbation since they believed that all lower-lying doublet states are strongly bound. They argued further that the potential curve of the interacting state must be very flat and proceed almost hori-

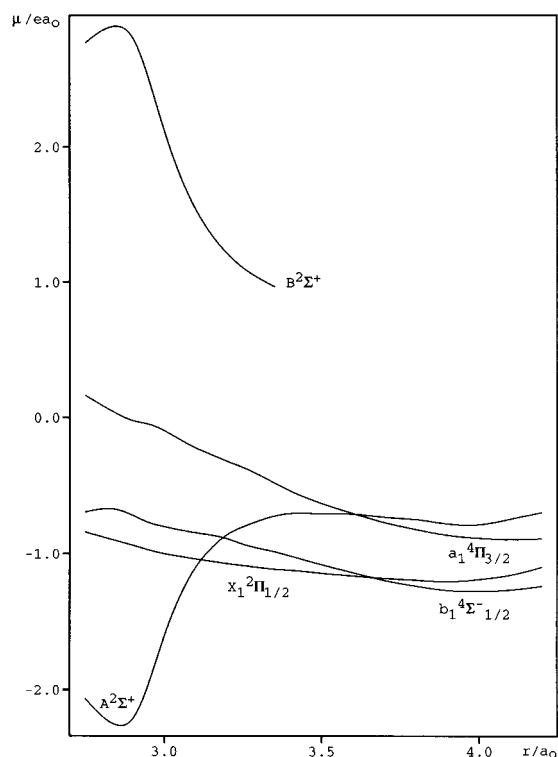


FIG. 7. Variation of the electric dipole moment of several low-lying states of the AsO molecule (a negative value corresponds to As^+O^- polarity). Results for the $B \ ^2\Sigma^+$ state are only given up to $r=3.4 a_0$, at which point a change of electronic configuration occurs.

zonally to its dissociation limit, which was thought to involve the ground state atomic levels $\text{As}(^4S_u) + \text{O}(^3P_g)$, because the onset of the intensity breakup occurs quite abruptly at a particular rotational level and the effect itself is rather weak.

The present calculations indicate quite clearly that this interpretation is incorrect, however, as can be judged from the potential curves of Figs. 1 and 2. Instead the true explanation seems to involve the $A\ ^2\Sigma^+$ state, with the key point being that its potential curve has a maximum near $r = 4.5\ a_0$ and its energy at that location is very close to the minimum value calculated for $B\ ^2\Sigma_{1/2}^+$. It is noteworthy that Meyer²⁴ has indicated in his work that the perturbing state should be of Σ^+ symmetry, consistent with the present interpretation. The onset of the B level perturbations occurs rather suddenly because of the need to pass over the $A\ ^2\Sigma^+$ barrier. Since the energy at the top of the barrier exceeds that of the lowest AsO dissociation limit by a significant margin, however, at least in the present calculations, it follows that the ground state D_0^0 is considerably less than the 4.980 eV value given as an upper limit for this quantity in Ref. 5. In our recent study of the SbO spectrum¹ a similar situation was noted for the experimental D_0^0 value for the ground state of this system. The convergence point of the present potential curves at the lowest dissociation limit is $32\ 500\ \text{cm}^{-1}$ and the aforementioned A -state barrier is roughly $6100\ \text{cm}^{-1}$, so the sum of $38\ 600\ \text{cm}^{-1}$ would correspond in this interpretation to the energy at which the onset should occur. Since the observed value is $40\ 650\ \text{cm}^{-1}$, it follows that there is an error of roughly $2000\ \text{cm}^{-1}$ or $0.25\ \text{eV}$ inherent in the present theoretical treatment. This would imply that the ground state D_e value is actually $34\ 500\ \text{cm}^{-1}$ or $4.28\ \text{eV}$, which would mean that the D_0^0 result deduced by Callomon and Morgan⁵ is probably too high by roughly $0.7\ \text{eV}$.

There has also been a thermodynamic measurement²⁶ of D_0^0 which is in good agreement with the original spectroscopic estimate, however. It is based on the determination of equilibrium constants for the oxygen-exchange reaction: $\text{As} + \text{SnO} \rightarrow \text{AsO} + \text{Sn}$. The measured change in the Gibbs energy function leads to a value for the average enthalpy change ΔH_{298}^0 of $12.1\ \text{kcal/mol}$. Combining this with an independent value for the $\text{SnO}\ D_0^0$ ($125.5\ \text{kcal/mol}$) implies an $\text{AsO}\ D_0^0$ value of $113.4 \pm 1.8\ \text{kcal/mol}$ or $4.92 \pm 0.08\ \text{eV}$. The very questionable assumptions underlying the original spectroscopic estimate for this quantity, particularly the existence of such weakly repulsive potential curves, indicate that the good agreement between it and the above thermodynamic result is simply fortuitous and that the error limits given in Ref. 26 should be reevaluated.

The highest-energy AsO states for which spectroscopic data are available are the $C_1\ ^2\Delta_{3/2}$ and $C_2\ ^2\Delta_{5/2}$, with T_e values near $40\ 000\ \text{cm}^{-1}$ (Table II). The present computed results are both too high by $1600\ \text{cm}^{-1}$. The spin-orbit energy splitting is relatively small, only $48\ \text{cm}^{-1}$ observed as compared to $35\ \text{cm}^{-1}$ computed. The $C\ ^2\Delta\ A-S$ state arises from the $\sigma \rightarrow \pi^*$ excitation and its measured r_e value is only $0.029\ \text{\AA}$ smaller than that for the $D\ ^2\Sigma^-$ of the same electronic configuration ($0.018\ \text{\AA}$ computed). Several perturbing electronic states exist, especially for the $\Omega = 3/2$ component

TABLE IV. Calculated radiative lifetimes of excited states of AsO ($v' = 0$): partial lifetimes τ_1 , τ_2 , and τ_3 for transitions to $X_1\ ^2\Pi_{1/2}$, $X_2\ ^2\Pi_{3/2}$, and $a\ ^4\Pi$, respectively, and total lifetime τ .

State	$\tau_1(\text{s})$	$\tau_2(\text{s})$	$\tau_3(\text{s})$	$\tau(\text{s})$
$X_2\ ^2\Pi_{3/2}$	12.2			12.2
$a_1\ ^4\Pi_{3/2}$	7.3×10^{-3}	3.7×10^{-3}		2.5×10^{-3}
$a_2\ ^4\Pi_{5/2}$		3.6×10^{-3}		3.6×10^{-3}
$a_3\ ^4\Pi_{1/2}$	1.5×10^{-3}	840×10^{-3}		1.5×10^{-3}
$a_4\ ^4\Pi_{1/2}$	58×10^{-3}	6.0×10^{-3}		5.4×10^{-3}
$G_1\ ^2\Pi_{3/2}$	10.8×10^{-3}	55.7×10^{-6}		55.4×10^{-6}
$G_2\ ^2\Pi_{1/2}$	48.7×10^{-6}	37×10^{-3}		48.6×10^{-6}
$b_1\ ^4\Sigma_{1/2}^-$	193×10^{-6}	556×10^{-6}	$17.5 \times 10^{-6}\ a$	8.2×10^{-6}
			17.2×10^{-6}	
$b_2\ ^4\Sigma_{3/2}^-$	3.6	160×10^{-6}	$19.4 \times 10^{-6}\ a$	8.7×10^{-6}
			17.5×10^{-6}	
$I_2\ ^2\Phi_{5/2}$		3.1×10^{-3}		3.1×10^{-3}
$A\ ^2\Sigma_{1/2}^+$	0.43×10^{-6}	0.45×10^{-6}		0.22×10^{-6}
$B\ ^2\Sigma_{1/2}^+$	0.42×10^{-7}	0.42×10^{-7}		0.21×10^{-7}
$D\ ^2\Sigma_{1/2}^+$	0.52×10^{-6}	0.95×10^{-6}		0.34×10^{-6}
$H_1\ ^2\Pi_{3/2}$	85.4×10^{-6}	8.8×10^{-6}		8.0×10^{-6}
$H_2\ ^2\Pi_{1/2}$	65.8×10^{-6}	188×10^{-6}		48.7×10^{-6}
$C_1\ ^2\Delta_{3/2}$	0.33×10^{-6}	13.9×10^{-6}		0.32×10^{-6}
$C_2\ ^2\Delta_{5/2}$		0.35×10^{-6}		0.35×10^{-6}

^aPartial lifetimes are given for transitions: (a) from $b_1\ ^4\Sigma_{1/2}^-$ to $a_1\ ^4\Pi_{3/2}$ and $a_3\ ^4\Pi_{1/2}$; (b) from $b_2\ ^4\Sigma_{3/2}^-$ to $a_2\ ^4\Pi_{5/2}$ and $a_4\ ^4\Pi_{1/2}$, respectively.

(Figs. 3 and 4). The sharply avoided crossing between H_1 and C_1 is expected to produce drastic changes in the transition probability to the $X\ ^2\Pi$ ground states, as will be discussed in the following section.

V. TRANSITION PROBABILITIES AND RADIATIVE LIFETIMES

The Born–Oppenheimer electronic and vibrational wave functions discussed above have been employed to compute transition probabilities from various AsO upper states to at least the $X_1\ ^2\Pi$ and $X_2\ ^2\Pi$ ground states. The corresponding radiative lifetimes for the $v' = 0$ levels are given in Table IV. The $X_2\ ^2\Pi_{3/2}$ lifetime itself is quite long and it has not yet been possible to measure it by the usual Stern–Vollmer technique. Only the electric dipole matrix element has been calculated, however, and so it may be necessary to consider higher-order multipole or magnetic-dipole results to obtain an accurate estimate for this quantity, but in all probability the true experimental value is on the order of a second or more. The corresponding SbO lifetime has been computed to be $0.29\ \text{s}$,¹ whereas the BiO analog has been measured to be $0.48\ \text{ms}$ ²⁷ (computed value, $2.7\ \text{ms}$ ²). No experimental values are available for the various $a\ ^4\Pi$ multiplets either, but the present calculations find that all four lifetimes fall in the ms region. The $\Omega = 5/2\ a_2\ ^4\Pi$ state should be detectable on the basis of the present computed transition probability between it and the X_2 state. Analysis of the calculated results shows that the combination of a small admixture of $^2\Sigma^\pm$ and $^2\Delta$ character to the $a\ ^4\Pi$ state and of $^4\Sigma^-$ to the $X\ ^2\Pi$ ground state is mainly responsible for the moderately large perpendicular dipole matrix elements computed. Parallel transitions occur primarily because of a $^4\Pi - ^2\Pi$ mixing in

the two adiabatic states. It is also interesting that the two $\Omega=1/2$ $a^4\Pi$ states have opposite preferences for the lower state in their respective transitions.

The $G^2\Pi$ radiative lifetimes are several orders of magnitude shorter and the corresponding transition probabilities show that the parallel mechanism is greatly preferred in this case. Both results are to be expected since $^2\Pi\text{--}^2\Pi$ dipole-allowed transitions are primarily responsible for the computed trends. The $b^4\Sigma^-$ lifetimes are about six times shorter than those for $G^2\Pi$ (Table IV), but this is clearly not because of transitions to $X^2\Pi$, rather to various $a^4\Pi$ multiplets. As a result ($\Delta\Lambda=\pm 1$) the preferred mechanism is found to be perpendicular. Such processes could be important in the experimental search for the $a^4\Pi$ states, but populating the $b^4\Sigma^-$ state is not easily accomplished, however, because of the proximity of the $G^2\Pi$ states (Figs. 2 and 3). The partial lifetime for $I_2^2\Phi_{5/2}\text{--}X_2^2\Pi_{3/2}$ is calculated to be 3.1 ms and its transition probability arises mainly from the small $^2\Delta$ admixture to both the $^2\Phi$ and $X^2\Pi$ states. The other $^2\Phi$ component has $\Omega=7/2$ and therefore transitions from this state to both ground state components are dipole forbidden.

The $A^2\Sigma_{1/2}^+$ has a shorter lifetime than any of its lower-energy counterparts. It undergoes transitions to the two $X^2\Pi$ components with almost equal probability, both via a perpendicular ($\Sigma\text{--}\Pi$) mechanism. The $B^2\Sigma_{1/2}^+$ state is similar in this respect, but has an order-of-magnitude shorter lifetime and undergoes the strongest downward transitions of any of the AsO electronic states studied. As noted in the previous section, the B state is strongly perturbed by a number of neighboring states. The $D^2\Sigma^-$ is also relatively short-lived (0.34 μs), but its transitions to X_1 are almost twice as probable according to the present calculations (perpendicular transitions are preferred). The $H^2\Pi$ states live significantly longer, especially H_2 , so the potential curve crossing with $D^2\Sigma^-$ can have a large effect on individual vibrational transition probabilities. It is clear from Table IV that parallel transitions to $X^2\Pi$ are preferred, especially for H_1 . These results help to explain why the (shorter-lived) H_1 state (Table II) has been detected experimentally, while H_2 has not. Finally, both C states have strong perpendicular ($\Delta\text{--}\Pi$) transition to the respective $X^2\Pi$ components. In contrast to the $H^2\Pi$ pair, the two C multiplets are computed to have nearly equal radiative lifetimes. Higher-lying AsO states will not be given further consideration, but it is clear that as the density of states increases, the importance of nonadiabatic effects grows and nonradiative transitions play a much stronger role than in the low-energy portion of the AsO spectrum.

VI. CONCLUSION

Spin-orbit CI calculations based on relativistic effective core potentials have been employed to obtain potential energy curves and transition probabilities for the low-lying electronic states of the AsO molecule. There have been a number of careful experimental studies of the electronic spectrum of this system and the present calculations find good agreement with all spectroscopic constants for states with T_e values up to 40 000 cm^{-1} . It is pointed out that the

first excited $\Lambda\text{--}S$ state is the $\pi\text{--}\pi^* a^4\Pi$ and experimental evidence supporting this result can be taken from a band system reported by Kushawaha *et al.*¹⁹ which was originally assigned to the $A''^2\Sigma^+\text{--}X^2\Pi$ transition. The G_1 and $G_2^2\Pi$ states of the same electronic configuration come next and their computed T_e values agree with the measured results to within 600 cm^{-1} , while errors in the corresponding r_e and ω_e values of ~ 0.01 Å and ~ 20 cm^{-1} are noted. The large difference between the r_e values of these states and their $X^2\Pi$ counterparts produces a distinctive pattern in the associated vibrational intensity distribution which is nearly quantitatively reproduced in the present calculations. The b_1 and $b_2^4\Sigma^-$ states are next in energetic order, but it is not clear whether they correspond to the experimental F and L states, especially since the energy splitting computed for them is much smaller than the observed $F\text{--}L$ T_e value difference.

The $A^2\Sigma_{1/2}^+$ state is computed to have strong perpendicular transitions to both X_2 and X_1 and to be perturbed by both the G_2 and b_1 states. The $I^2\Phi$ states with $\Omega=7/2$ and $5/2$ are found to have slightly smaller T_e values than $A^2\Sigma^+$, and the intensity calculations indicate that the transition from the $5/2$ component to $X^2\Pi_{3/2}$ can be observed. After this there is a gap in T_e values of over 5000 cm^{-1} , at which point the $H^2\Pi$, $D^2\Sigma^-$, $B^2\Sigma^+$, and $C^2\Delta$ states come into play. The B state turns out to be a nearly pure Rydberg state in the Franck–Condon region of the ground state and is the only one of the low-lying states to possess As^-O^+ polarity. There is a sharp onset for its high- N $v'=0$ rotational levels for nonradiative transitions. The present calculations indicate that this phenomenon is caused by the presence of a barrier in the $A^2\Sigma^+$ potential curve whose maximum coincides with the energy of the above rotational levels on this basis. It appears that the D_0^0 value for the $X^2\Pi$ AsO ground state lies in the 4.2–4.3 eV area, rather than near 4.9 eV as originally proposed on the basis of assumed characteristics for the potential curves of perturbing states which are unrealistic according to the present work. The last states considered are the $C_1^2\Delta_{3/2}$ and $C_2^2\Delta_{5/2}$ arising from the $\sigma\text{--}\pi^*$ excitation. Their calculated T_e values overestimate the observed values by 1600 cm^{-1} or 0.2 eV, the largest such discrepancy in the present study. Comparison of these results with those computed in an analogous manner for the heavier Group V oxides, SbO and BiO, allows for a systematic evaluation of the increasing role of relativistic effects, especially spin-orbit coupling, with increasing atomic number of the heavier nucleus.

ACKNOWLEDGMENTS

One of us (A.B.A.) would like to thank the Alexander von Humboldt Foundation for the granting of a stipend, while another of us (A.B.S.) wishes to thank the Deutsche Forschungsgemeinschaft for support enabling him to visit the University of Wuppertal for a period of three months within the Forschergruppe “Erzeugung, Nachweis und Eigenschaften reaktiver Moleküle.” The financial support of the Fonds der Chemischen Industrie is also hereby gratefully acknowledged.

- ¹A. B. Alekseyev, H.-P. Liebermann, R. J. Buenker, and G. Hirsch, *J. Chem. Phys.* **102**, 2539 (1995).
- ²A. B. Alekseyev, H.-P. Liebermann, R. J. Buenker, G. Hirsch, and Y. Li, *J. Chem. Phys.* **100**, 8956 (1994).
- ³S. B. Rai and D. K. Rai, *Chem. Rev.* **84**, 73 (1984).
- ⁴K. P. Huber and G. Herzberg, *Molecular Spectra and Molecular Structure, Vol. 4, Constants of Diatomic Molecules* (Van Nostrand Reinhold, Princeton, 1979).
- ⁵J. H. Callomon and J. E. Morgan, *Proc. Phys. Soc. (London)* **86**, 1091 (1965).
- ⁶S. Mrozowski and C. Santaram, *J. Opt. Soc. Am.* **56**, 1174 (1966).
- ⁷M. M. Hurley, L. F. Pacios, P. A. Christiansen, R. B. Ross, and W. C. Ermler, *J. Chem. Phys.* **84**, 6840 (1986).
- ⁸L. F. Pacios and P. A. Christiansen, *J. Chem. Phys.* **82**, 2664 (1985).
- ⁹W. H. E. Schwarz and R. J. Buenker, *Chem. Phys.* **13**, 153 (1976).
- ¹⁰R. J. Buenker and S. D. Peyerimhoff, *Theor. Chim. Acta* **35**, 33 (1974); **39**, 217 (1975); R. J. Buenker, S. D. Peyerimhoff, and W. Butscher, *Mol. Phys.* **35**, 771 (1978).
- ¹¹R. J. Buenker and R. A. Phillips, *J. Mol. Struct. (THEOCHEM)* **123**, 291 (1985).
- ¹²E. R. Davidson, in *The World of Quantum Chemistry*, edited by R. Daudel and B. Pullman (Reidel, Dordrecht, 1974), p. 17.
- ¹³G. Hirsch, P. J. Bruna, S. D. Peyerimhoff, and R. J. Buenker, *Chem. Phys. Lett.* **52**, 442 (1977).
- ¹⁴R. J. Buenker, D. B. Knowles, S. N. Rai, G. Hirsch, K. Bhanuprakash, and J. R. Alvarez-Collado, in *Studies in Physical and Theoretical Chemistry, Vol. 62, Quantum-Chemistry—Basic Aspects, Actual Trends*, edited by R. Carbó (Elsevier, Amsterdam, 1989), p. 181.
- ¹⁵D. B. Knowles, J. R. Alvarez-Collado, G. Hirsch, and R. J. Buenker, *J. Chem. Phys.* **92**, 585 (1990).
- ¹⁶J. W. Cooley, *Math. Comput.* **15**, 363 (1961).
- ¹⁷M. Perić, R. Runau, J. Römelt, S. D. Peyerimhoff, and R. J. Buenker, *J. Mol. Spectrosc.* **78**, 309 (1979).
- ¹⁸S. A. Jarret-Sprague and I. H. Hillier, *Chem. Phys.* **148**, 325 (1990).
- ¹⁹V. S. Kushawaha, B. P. Asthana, and C. M. Pathak, *J. Mol. Spectrosc.* **41**, 577 (1972).
- ²⁰V. M. Anderson and J. H. Callomon, *J. Phys. B* **6**, 1664 (1973).
- ²¹J. P. Gouere, J. Figuet, J. N. Massot, and J. d'Incan, *Can. J. Phys.* **50**, 1926 (1972).
- ²²M. Venkataramaiah and S. V. Lakshman, *Indian J. Phys.* **38**, 209 (1960).
- ²³M. Chergui, N. Schwentner, and V. Chandrasekharan, *J. Chem. Phys.* **89**, 7094 (1988).
- ²⁴B. Meyer, *J. Mol. Spectrosc.* **18**, 443 (1965).
- ²⁵F. C. Connelly, *Proc. Phys. Soc.* **46**, 790 (1934).
- ²⁶K. H. Lau, R. D. Brittain, and D. L. Hildenbrand, *Chem. Phys. Lett.* **81**, 227 (1981).
- ²⁷E. H. Fink and O. D. Shestakov (private communication).